New family of fluorogenic azacrown probes with identical cavity size but different electronic environment outside the macrocycle: Effects on sensitivity of Cu2+ detection

ARTICLE *in* JOURNAL OF INCLUSION PHENOMENA AND MACROCYCLIC CHEMISTRY · SEPTEMBER 2014

Impact Factor: 1.43 · DOI: 10.1007/s10847-014-0453-z

3 AUTHORS:

Anita Pandey

Indian Institute of Technology Bombay

7 PUBLICATIONS **11** CITATIONS

SEE PROFILE

Raghuvir R S Pissurlenkar

Bombay College of Pharmacy

42 PUBLICATIONS **296** CITATIONS

SEE PROFILE

Anil Karnik

University of Mumbai

40 PUBLICATIONS **225** CITATIONS

SEE PROFILE

J Incl Phenom Macrocycl Chem
DOI 10.1007/s10847-014-0453-z

SHORT COMMUNICATION

New family of fluorogenic azacrown probes with identical cavity size but different electronic environment outside the macrocycle: effects on sensitivity of Cu^{2+} detection

Anita D. Pandey · Raghuvir R. S. Pissurlenkar · Anil V. Karnik

Received: 7 June 2014 / Accepted: 12 September 2014

Abstract Benzimidazoles derived from lactic acid and mandelic acid were employed as photosignaling synthons to construct 15-C-5 azacrowns **3** & **4** with difference in electronic environments at the carbon attached to 2-position. These receptors were used as probes for cation sensing using UV–Vis and fluorescence titration techniques. Although both the receptors have identical macrocyclic backbone and are found selective for Cu^{2+}, receptor **3** displayed stronger binding towards Cu^{2+} in comparison to **4**. The addition of Cu^{2+} to the probes **3** & **4** in solution caused quenching of fluorescence. The results clearly indicate that the stability of Cu^{2+} complexes of **3** and **4** depends on different factors. The association constant, K_{SV} for **3** with Cu^{2+} was (1.53×10^5 M^{-1}) an order higher than that exhibited by **4** for Cu^{2+} (9.27×10^4 M^{-1}).

Keywords Benzimidazole · Azacrown · Semi-rigidity · Fluorescent sensors · Copper

Introduction

Receptor design finds its basis in variety of factors like conformational rigidity, conformational landscape offered by the receptor, architectural preorganization, symmetry, presence of chromophores for optical signaling, additional binding sites etc. [1, 2]. Selective binding domains tagged with optical probes lead to signature optical response due to perturbed photophysical properties upon analyte association. Benzofused heterocycles are appropriate motifs for tagging optical sensors due to their versatility in terms of freedom of structural tuning, enhanced π-π- interactions and availability of heteroatom's. Several bioreceptors contain heterocycles in their backbone like purines, pyrimidines, azoles etc. [3, 4]. Few azacrown receptors with heterocycle as an intrinsic part of macrocyclic backbone are reported [5, 6]. The recent years have witnessed extensive development of several fluorescent sensors for metal ions of biological, clinical or environmental significance like Na^+, Ca^{2+}, Cu^{2+}, Zn^{2+} etc. [7–11]. After Fe^{2+} and Zn^{2+}. Cu^{2+} is the third abundant transition metal ion found in vivo and its existence in balanced amount is crucial for smooth functioning of physiological system [12–16]. Imbalance in levels of Cu^{2+} results in increased risk of coronary heart diseases. Cu^{2+} participates in reactions producing reactive oxygen species causing lethal cellular conditions like lipid peroxidation and DNA damage due to its redox nature [17]. Excessive amounts of Cu^{2+} is environmental pollutant and can cause neurodegenerative diseases like Parkinson's, Alzheimer's, Wilson's etc. [18, 19]. Cu^{2+} being a biologically significant cation with important biomedical implications, there is considerable interest in developing selective and sensitive copper sensors. Sensors detecting Cu^{2+} in water, especially at physiological pH with convenient signal detection are in

Electronic supplementary material The online version of this article (doi:10.1007/s10847-014-0453-z) contains supplementary material, which is available to authorized users.

A. D. Pandey · A. V. Karnik (✉)
Department of Chemistry, University of Mumbai, Vidyanagari, Santacruz (East), Mumbai 400098, India
e-mail: avkarnik@chem.mu.ac.in

R. R. S. Pissurlenkar
Department of Pharmaceutical Chemistry, Bombay College of Pharmacy, Molecular Simulations Group, Kalina, Santacruz (East), Mumbai- 400098, India

Published online: 21 September 2014

high demand [20–32]. In the present article we report 15-[C]-5-azacrown metal sensors derived from two different benzimidazoles, performing as fluorescence "*Turn-off*" Cu^{2+} sensors with varying sensitivity subject to different conformational landscapes offered.

Background

Our active investigations in structural tuning of benzimidazole architecture have provided access to synthons with interesting ligating properties finding applications as chiral auxiliaries, tweezers, catalysts, ionic liquids for green synthesis etc. [33–35]. Recently we reported 2-(α-hydroxyethyl) benzimidazole, **(1)** derived 15-C-5-azacrown **(3)** as a selective chiral sensor for *S*-(-)-enantiomers of biologically important amines [36]. Azolide derived from **1,** have been successfully employed by us [37, 38] and Katritzky et al. for kinetic resolution studies [39]. 2-(α-Hydroxy alk/aryl) benzimidazoles can be conveniently obtained by a single step reaction between o-phenylenediamine and the corresponding α-hydroxy acid [40, 41]. These molecules offer β-hydroxy amino moiety, which has been used extensively for construction of several aza-crowns [42–49]. The most interesting structural attribute of our sensor systems **3** and **4**, was branded by the presence of benzimidazole as an integral part of macrocyclic cavity. We intended to envisage the semi-rigidity imparted to the benzimidazole-derived aza-crown cavity upon introduction of alkyl/aryl substituents close to the benzimidazole unit towards metal sensing.

Thus benzimidazole derived azacrowns **3** and **4** were synthesized and explored as cation sensors by studying the effect of various metal ions on its photophysical properties. A highly strained, electron rich region existing near the benzimidazole unit and aza-crown cavity due to a mutually shared C–N bond, could be easily perturbed with the existence of metal ion in the vicinity. It was also of interest to observe the impact of switching between substituents from aliphatic to aromatic at 2-position of benzimidazole, on selectivity and sensitivity. The blending of recognition ability by the crown part and fluorescence signaling by the benzimidazole motifs enabled observation and quantification of guest ion upon its introduction to receptors using electronic absorption and fluorescence spectroscopy.

Results and discussion

2-(α-hydroxyethyl)benzimidazole [HEB] (**1**) and 2-(α-hydroxybenzyl)benzimidazole [HBB] **(2)** were obtained from lactic acid and mandelic acid respectively. Syntheses of **3** and **4** was readily achieved by coupling of tetra ethylene glycol ditosylate with **1** and **2**, in presence of a sodium hydride as a base under high dilution conditions in inert atmosphere. Workup and chromatographic purification afforded receptors **3** (48 %) and **4** (50 %) dilution conditions in inert atmosphere (Scheme 1). Compounds **3** and **4** were characterized by the usual spectroscopic and analytical techniques, IR, ^{1}H and ^{13}C NMR, 2-D NMR, ESI–MS, elemental analysis etc.

To our delight receptor **3** was a solid, hence good quality crystals were prepared for XRD studies. Single crystal XRD analysis of mono aza-crown **3** confirmed the structure of receptor **3** and revealed that the benzimidazole backbone provided conformational rigidity to the crown cavity, while the portion of macrocycle away from the heteroalkyl ring exhibited two major conformations [36]. On the contrary receptor **4** was obtained as a viscous oil and single crystal XRD could not be studied for this compound.

The rigidity imparted to macrocyclic backbone invokes selectivity in guest association and optical signaling. Single crystal XRD structure of receptor **3** exhibited a partially rigid nature of the portion of macrocycle formed due to the benzimidazole motif, offering the desired conformational stability and the remaining portion displayed conformational mobility (see supplementary information, figure SI-25). One of the nitrogen atoms, N-2 from the benzimidazole ring along with the hydroxyl substituent present at the α-carbon are involved in the formation of azacrown macrocycle. The C–N bond between N-2 nitrogen and C-7 carbon exists commonly shared by the azole ring as well as the crown cavity, providing a rigid geometry in this region of the macrocycle. Moreover the N-1 nitrogen atom appears as a hydrate in the single crystal X-ray ascertaining its involvement in complexation with metal ion guest by donation of the electron lone pair. The other most proximal donor atom was the O-1 oxygen atom provided by the benzimidazole backbone itself, which could ideally assist in complexation.

The design concept relies on the rationale that metal ion coordination with **3** and **4** would involve tripodal cation-bonded interaction with the N-1 nitrogen of benzimidazole, O-1 oxygen atom present at C-8 or α-carbon along with the third nearest donor atom O-2 offered by the aza-crown ring.

The difference in strength of the receptor-cation complex formed by **3** and **4** would depend upon the conformational landscape offered at α carbon atom with respect to benzimidazole ring, due to the nature of substituent present (Fig. 1a, b).

The difference in optical response of receptors **3** and **4** upon forming an inclusion complex with metal ions could be accounted to the dissimilar steric/electronic environment proximal to the benzimidazole motif present in the semi-rigid portion of the aza-crown (Fig. 2). The dissimilar optical response of metal complexes of **3** and **4** towards photophysical perturbations attracted us to harness their potential in metal sensing applications.

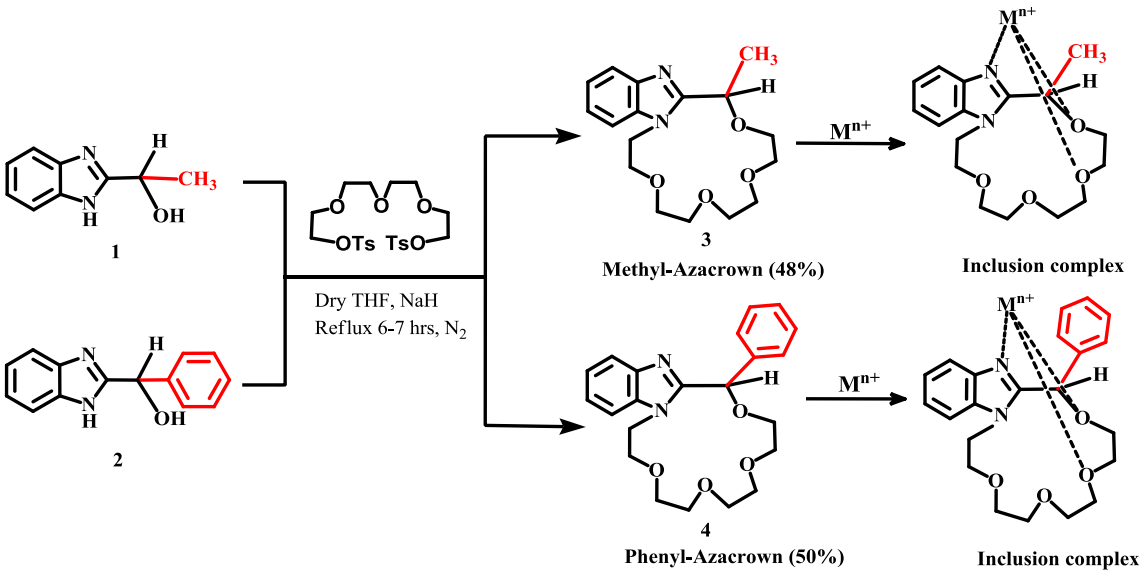

Scheme 1 Synthesis of azacrown receptors **3** and **4** and their interaction with cations

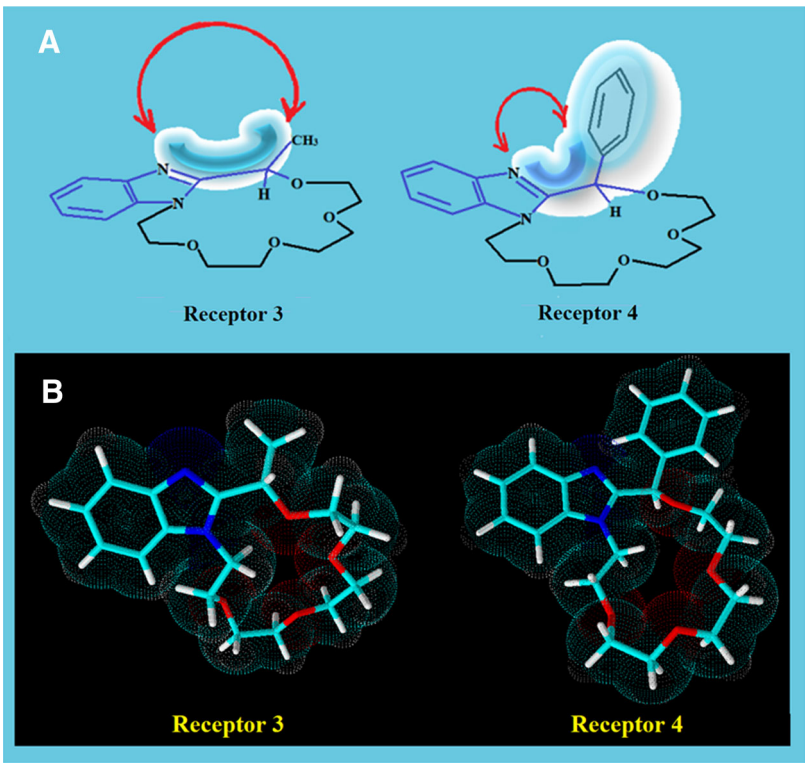

Fig. 1 **a** Model and **b** 3D optimized structure showing electron cloud arrangement around azacrown receptors **3** & **4**

Materials and methods

Absorption spectra were recorded on Shimadzu UV–Vis Spectrophotometer UV-2100. Emission spectra were obtained on a Perkin-Elmer LS-55 spectrofluorimeter. In order to allow comparison of emission intensities, corrections for inner filter effects were performed. Degassed solvents were used and absorbance and emission spectra were obtained at 298 K.

UV–Vis and fluorescence spectroscopic studies

The optical sensitivity of aza-crowns 3 and 4 towards metal ions was evaluated by both absorbance and fluorescence

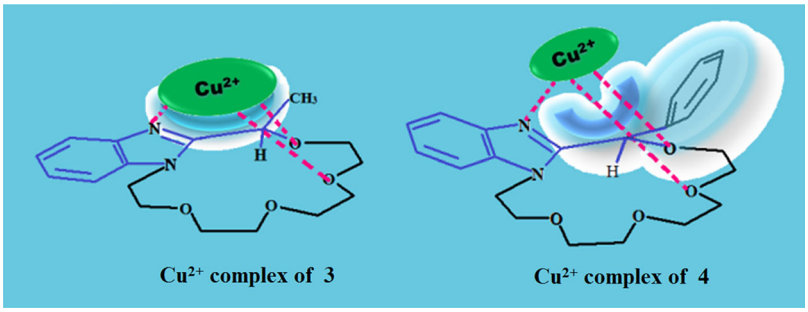

Fig. 2 Conformational landscape offered by azacrowns **3** & **4** during complexation

spectral techniques. The design principle of these receptors is based on the premise that the analyte/cation chelation via N–O–O coordination with receptor aza-crowns would induce enhanced charge transfer thereby producing detectable changes in optical properties of receptor. Metal ions of biological and environmental interest like Li^+, Na^+, Ba^{2+}, Ca^{2+}, Cd^{2+}, Co^{2+}, Cu^{2+}, Mg^{2+}, Ni^{2+} and Zn^{2+}; were investigated for the complexation induced photophysical effects on intrinsic spectral properties of receptors **3** and **4**. Titration experiments were carried out systematically with a set of 10 metal ions, for both the receptors **3** and **4** individually, by adding the solutions of metal perchlorates in MeCN to a solution of host receptors **3** and **4** in H_2O–MeCN (9:1 v/v buffered by 10 mM HEPES buffer, pH 7.2 ± 0.1; further references will be made as; buffer).

In the UV–Vis spectrum of receptors **3** and **4** in free and complexed forms, neither the extinction coefficient nor the wavelength of absorption changed significantly in the presence of all the metal salts except copper. A small red-shift of the absorption maximum (~3–5 nm) was observed with the majority of the metal salts. In almost all the cases, no isobestic point could be observed. The effect of the metal ions was however much more pronounced on the fluorescence behavior of the complexed systems. Addition of the metal salts resulted in larger Stokes shift of the fluorescence maximum (~52 nm), accompanied with quenching of the fluorescence intensity.

The UV–Vis spectrum of both **3** and **4** in buffer displayed structureless band with a strong absorbance at 206 nm due to $n \rightarrow \pi^*$ transitions attributed to C=N bond of imidazole ring and another comparatively weaker absorbance at 254 nm, assignable to $\pi \rightarrow \pi^*$ transitions associated to aromatic subunits. The molar extinction coefficient (ϵ) at 206 nm was (3.84×10^4 $M^{-1}cm^{-1}$) and at 254 nm was (6.9×10^3 $M^{-1}cm^{-1}$) for **3**, whereas molar extinction coefficient (ϵ) at 210 nm was (3.93×10^4 $M^{-1}cm^{-1}$) and at 254 nm was (7.37×10^3 $M^{-1}cm^{-1}$) for **4** respectively in buffer. Figure 3a shows the change in UV–Vis spectral response of **3** in free form and in the company of Li^+, Na^+, Ba^{2+}, Ca^{2+}, Cu^{2+}, Cd^{2+}, Co^{2+}, Mg^{2+}, Ni^{2+} and Zn^{2+} as their perchlorate salts. It was noted that addition of up to 200 equivalents of Li^+, Na^+, Ba^{2+}, Ca^{2+}, Cd^{2+}, Co^{2+}, Cu^{2+}, Mg^{2+}, Ni^{2+} and Zn^{2+} displayed negligible change in UV–Vis profile of **3**, In contrast addition of just 11 equivalents of Cu^{2+} to a solution of **3**, showed maximum increase in absorbance at 254 nm. It is clear that in comparison to other metal ions examined, only Cu^{2+} exhibited significantly pronounced response in the UV–Vis spectrum of **3** at the wavelength 254 nm.

The spectrophotometric titration of a fixed concentration of **3** (2.835×10^{-5} M) in buffer with an incremental addition of $Cu(ClO_4)_2$ (0–3.12×10^{-4} M) is depicted in the inset (Fig. 3b) indicating a progressively enhanced absorbance at 254 nm. After a limiting concentration of (3.12×10^{-4} M) of Cu^{2+} there was no considerable change in the absorption profile of **3**.

Figure 3c shows the change in UV–Vis spectral response of **4** in uncomplexed form and in the company of earlier mentioned metal ions as their perchlorate salts.

It was noticed that addition of up to 200 equivalents of Li^+, Na^+, Ba^{2+}, Ca^{2+}, Cd^{2+}, Co^{2+}, Cu^{2+}, Mg^{2+}, Ni^{2+} and Zn^{2+} displayed negligible change in UV–Vis profile of **3**, In contrast addition of just 20 equivalents of Cu^{2+} to a solution of **4** in buffer, showed maximum increase in absorbance at 254 nm.

Thus like receptor **3**, receptor **4** too exhibited selective response for Cu^{2+} in comparison to other metal ions in the UV–Vis spectrum of **4** at 254 nm. Figure 3 (*inset* d) depicts the spectrophotometric titration of **4** (5.67×10^{-5} M, buffer) with an incremental addition of $Cu(ClO_4)_2$ (0–$1.13 \times 10^{-}3$ M) indicating a progressively enhanced absorbance at 254 nm. After a limiting concentration of (0–1.13×10^{-3} M) of Cu^{2+} there was no considerable change in the absorption profile of **4**.

Fluorescence spectral changes of **3** and **4** before and after addition of Li^+, Na^+, Ba^{2+}, Ca^{2+}, Cd^{2+}, Co^{2+}, Mg^{2+}, Ni^{2+}, Zn^{2+} and Cu^{2+} are depicted in Fig. 4a, B respectively. When excited at 254 nm, receptor **3** emitted at 306 nm (λ_{em}) with a quantum yield Φ_f of 0.105 [53–55], exhibiting a substantial stokes shift of ~ 52 nm. The λ_{em} was unaltered upon addition of Li^+, Na^+, Ba^{2+}, Ca^{2+}, Cd^{2+}, Co^{2+}, Mg^{2+}, Ni^{2+} and Zn^{2+} up to (5.0×10^{-4} M) but 10–31 % quenching was observed (Fig. 4b).

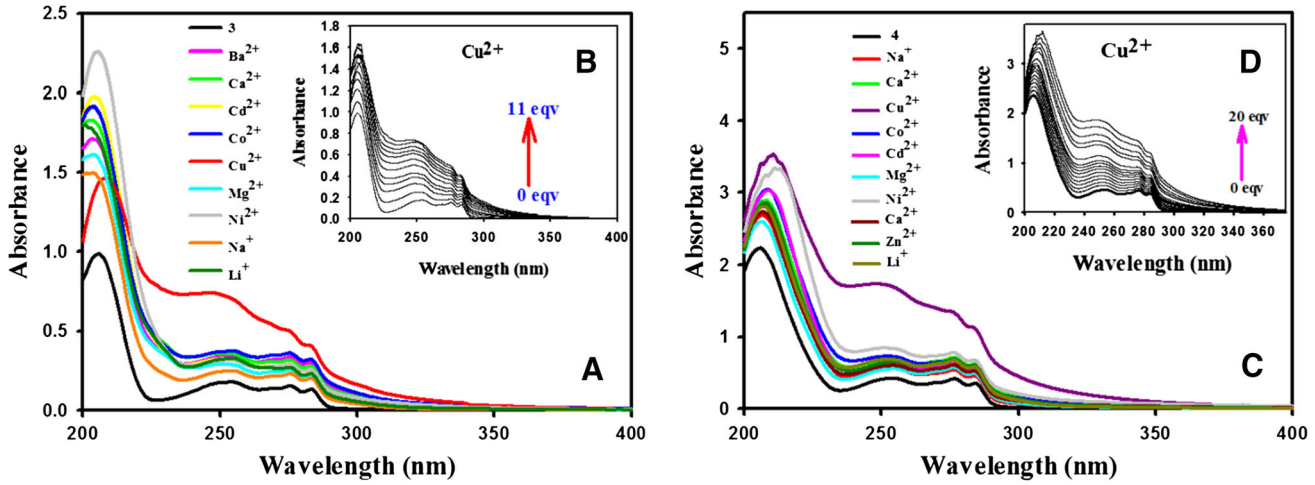

Fig. 3 **a** Absorption spectrum of **3** (2.835×10^{-5} M) in the absence and presence of perchlorates of Cu^{2+} (3.12×10^{-4} M) and Li^{+}, Na^{+}, Ba^{2+}, Ca^{2+}, Cd^{2+}, Co^{2+}, Mg^{2+}, Ni^{2+}, Zn^{2+} (5.67×10^{-3} M) in buffer (pH 7.2 ± 0.1) solution **b** Spectrophotometric titration of **3** with Cu^{2+} **c** Fluorescence spectra of **3** (1×10^{-6} M) in the absence and presence of Cu^{2+} (11×10^{-6} M) and other metal perchlorates (5×10^{-4} M) in buffer **d** Spectrophotometric titration of **4** with Cu^{2+}

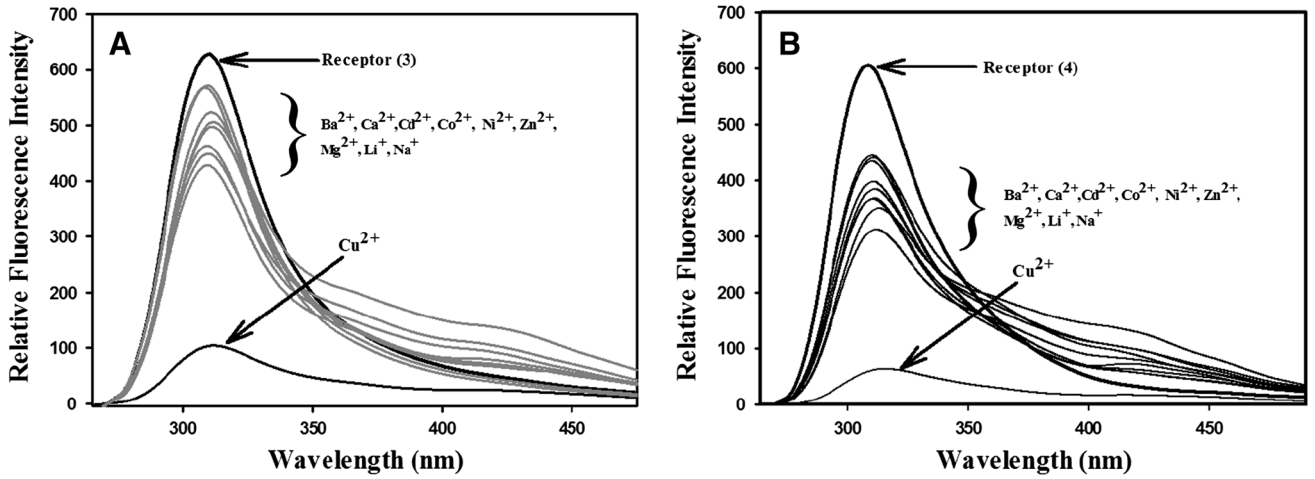

Fig. 4 **a** Fluorescence spectra of **3** (1×10^{-6} M) in the absence and presence of Cu^{2+} (11×10^{-6} M) and other metal perchlorates (5×10^{-4} M) in buffer **b** Fluorescence spectra of **4** (2×10^{-6} M) in the absence and presence of perchlorates of Cu^{2+} (4×10^{-5} M) and Li^{+}, Na^{+}, Ba^{2+}, Ca^{2+}, Cd^{2+}, Co^{2+}, Mg^{2+}, Ni^{2+}, Zn^{2+} (8×10^{-3} M) in buffer (pH 7.2 ± 0.1)

Thus both UV–Vis and fluorescence studies suggested insignificant binding of these metals with **3**. However Cu^{2+} (at $\lambda_{em} = 306$ nm) brought about substantial CHEQ (chelation enhanced emission quenching) up to 84 % with a slight red shift (~3 nm) (Fig. 4a). The Job's plot analysis of the fluorescence titration profile shows the existence of receptors **3** with Cu^{2+} in 1:1 stoichiometry in solution.

Similarly the receptor **4**, when excited at 254 nm, emitted at 309 nm (λ_{em}) with a quantum yield Φ_f of 0.126 and exhibiting a large stokes shift of ~55 nm. Addition of the metal ions did not vary the λ_{em} of receptor **4**, Li^{+}, Na^{+}, Ba^{2+}, Ca^{2+}, Cd^{2+}, Co^{2+}, Mg^{2+}, Ni^{2+} and Zn^{2+} up to 400 eqv (8×10^{-3} M) but 26–48 % quenching was observed, thus both UV–Vis and fluorescence studies suggested poor binding of these metals with **4**, except for Cu^{2+} which brought about dramatic chelation enhanced emission quenching (CHEQ) up to 90 % with λ_{em} red shifted from 303 to 309 nm (~6 nm) (Fig. 4b). The Job's plot analysis of the fluorescence titration profile shows the existence of receptors **4** with Cu^{2+} in 1:1 stoichiometry in solution. Thus both the aza-crowns **3** and **4** both displayed high selectivity for Cu^{2+} ions.

For fluorescence quenching titration measurements, **3** (1×10^{-6} M) was titrated with varying concentrations of alkali and alkaline earth metal ions (0–5×10^{-4} M) in buffer at 25 °C. The samples were excited at 254 nm, and

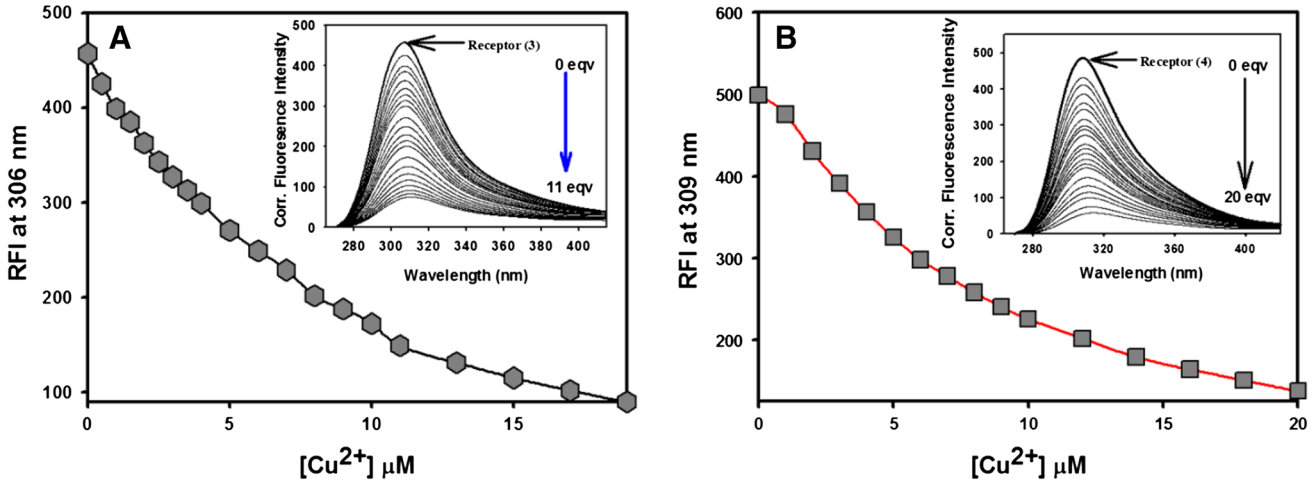

Fig. 5 **a** Spectrofluorometric titration of **3** (1×10^{-6} M) with $Cu(ClO_4)_2$ (2.2×10^{-6} M) in buffer (pH 7.2 ± 0.1) **b** Spectrofluorometric titration of **4** (2×10^{-6} M) with $Cu(ClO_4)_2$ (4×10^{-5} M) in buffer (pH 7.2 ± 0.1)

the fluorescence emission was recorded from 264 to 500 nm. The excitation and emission slits were set at 5 nm (Fig. 5a).

The fluorescence intensities were corrected for inner filter effects of receptors and analyte using Eq. 1 [50]

$$F_{corr} = F_{obs}.10^{(OD_{ex}+OD_{em})/2} \quad (1)$$

where F_{corr} and F_{obs} are the corrected and observed fluorescence intensities, OD_{ex} and OD_{em} are the optical densities of receptors in presence of analyte at the excitation and emission wavelengths, respectively. The average of OD_{ex} and OD_{em} for receptors **3** and **4** and metal ions lay in the range from 0.02 to 0.43.

The emission spectrum of **3** showed a quenching of emission intensity at 306 nm when excited at 254 nm. Addition of different metal ions Li^+, Na^+, K^+, Ba^{2+}, Ca^{2+}, Mg^{2+}, Cd^{2+}, Zn^{2+}, Co^{2+} and Ni^{2+} to the solution of **3** induced varying degrees of emission quenching depending on the identity of the metal ion. Figure 5a exhibits the variation of emission intensities of **3** at 306 nm, as a function of increasing concentration of Cu^{2+}, in buffer.

Similarly fluorescence quenching titration measurements for receptor **4** (2×10^{-6} M) with varying concentrations of alkali and alkaline earth metal ions (0–8 $\times 10^{-3}$ M) in buffer at 25 °C were carried out. The samples were excited at 254 nm, and the fluorescence emission was recorded from 264 to 500 nm. The excitation and emission slits were set at 5 nm. Figure 5b exhibits the variation of emission intensities of **4** at 309 nm, as a function of increasing concentration of Cu^{2+}, in buffer.

The binding constant values were determined from the Stern–Volmer relation by plotting of F_0/F as a function of varying concentration of the Cu^{2+} (Eq. 2) [51, 52]

$$\frac{F_0}{F} = 1 + Ksv[Q] \quad (2)$$

The azacrown-cation complex parameters, association constant (Ka) and stoichiometry of binding (n) were determined by the modified double log Stern–Volmer equation (Eq. 3)

$$\log\left(\frac{F_0}{F} - 1\right) = \log Ka + n\log[Q] \quad (3)$$

Where F_0 and F are the fluorescence intensities in the absence and presence of quencher [Q], K_{sv} and K_a are the Stern–Volmer quenching and association constant, respectively. Slope and the intercept of plot log (Fo/F−1) Vs log[Q] gave n, which is number of binding sites present in the receptor, and was found to be ~1 in cases of all the metals for both **3** and **4**

Typical Stern–Volmer plots for spectrofluorometric titration of receptors **3** and **4**, are presented in Fig. 6.

The binding constant values for alkali metal ions were found to be lower than alkaline-earth metal ions. In agreement with the trend followed by simple aza-15-crown-5, the stability constants for alkaline earth metals exhibit the binding order as $Ca^{2+} > Ba^{2+} > Mg^{2+}$ for **3**. However in case of **4**, emission enhancements follow a different order of stability constants as being $Ca^{2+} > Mg^{2+} > Ba^{2+}$. The Stern–Volmer constant (K_{sv}), for **3** with various metal ions studied follow the order $Cu^{2+} > Ca^{2+} > Cd^{2+} > Ba^{2+} > Ni^{2+} > Li^+ > Co^{2+} > Zn^{2+} > Na^+ > Mg^{2+}$. Whereas K_{sv} for **4** displayed the following order $Cu^{2+} > Na^+ > Ca^{2+} > Li^+ > Co^{2+} > Zn^{2+} > Cd^{2+} > Mg^{2+} > Ba^{2+} > Ni^{2+}$.

From the UV–Vis and emission data and higher stability constant, we can conclude that chemosensor **3** and **4**

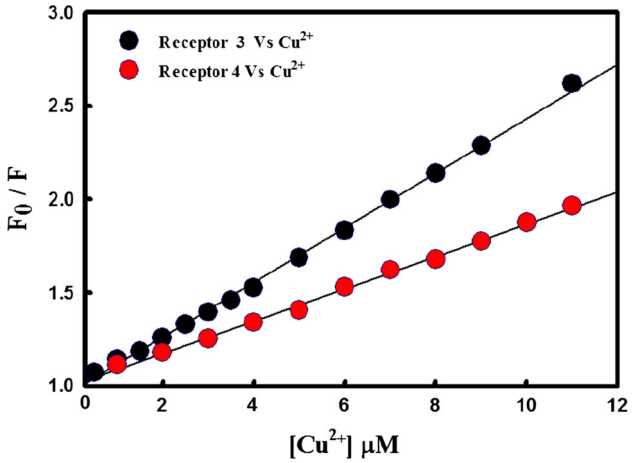

Fig. 6 Stern–Volmer plots for spectrofluorometric titration of receptors **3** and **4** with Cu^{2+} perchlorate

manifest highly selective binding with Cu^{2+} compared to alkali and alkaline-earth metal ions investigated. Benzimidazole has two nitrogen atoms, one pyridine type and the other pyrrole type, both can be considered to be comparatively soft and hence benzimidazole derived azacrowns contribute to binding with Cu^{2+} selectively. Good agreements are found in the stability constants K obtained by spectrophotometric titration and association constant K_a, obtained by spectrofluorometric titration (Table 1). Cu^{2+} based "*turn-off*" chemosensors are well reported [56–69], the present article describes the effect of difference in steric environment outside the receptor cavity playing a decisive role in extent of binding; with the core cavity size and ring composition remaining constant.

A maximum perturbation of the absorption spectrum together with a prominent quenching by Cu^{2+} supports its strong affinity for probes **3** and **4**, relative to the other metal ions tested. From the fluorimetric titrations, the detection limit of receptor **3** for Cu^{2+} was calculated to be 4.1×10^{-7} M and receptor **4** for Cu^{2+} to be 8.1×10^{-7} M, which is comparable with the values reported for several Cu^{2+} selective sensors [56–69].

The receptor systems **3** & **4**, we studied, appears to exhibit chelation induced quenching (CHEQ effect). To eradicate any ambiguity, the data acquired by spectrofluorometric titrations were corrected for inner-filter effects according to equation-1.

Dynamic quenching effects become apparent when quencher and the receptor undergo collisions in the excited state, hence ground state interactions ideally should not exhibit changes in the absorption spectra whereas static quenching process affects the ground state of the fluorophore [70]. In our case, the spectrophotometric titrations of the receptors **3** & **4** in the presence of Cu^{2+} showed that,

Table 1 Stern-Volmer constant (K_{sv}) and association constant (K_a) calculated from spectrofluorometric titrations, association constant (K) calculated using spectrophotometric titrations, Experimental free energy (ΔG_0), calculated free energies (E_h) and fluorescence quantum yield (Φ_f) of **3** and **4** in the presence of metal ions

	Aza-crown (3)						Aza-crown (4)					
Metal ion	$K_{sv} \times 10^4$ (M^{-1})	$K_a \times 10^5$ (M^{-1})	$K \times 10^4$ (M^{-1})	$-\Delta G_0$ (kJ mol^{-1})	E_h Hartrees	Φ_f	$K_{sv} \times 10^4$ (M^{-1})	$K_a \times 10^5$ (M^{-1})	$K \times 10^4$ (M^{-1})	$-\Delta G_0$ (kJ mol^{-1})	E_h Hartrees	Φ_f
Free	–	–	–	–	–	0.105	–	–	–	–	–	0.126
Ba^{2+}	3.32 (±) 0.01	0.05 (±) 0.11	1.28 (±) 0.02	25.79	−1097.54	0.075	1.17 (±) 0.05	0.02 (±) 0.06	0.74 (±) 0.04	23.22	−1289.28	0.091
Ca^{2+}	6.28 (±) 0.01	0.74 (±) 0.05	1.99 (±) 0.04	27.38	−1108.85	0.071	3.93 (±) 0.28	–	1.78 (±) 0.03	26.22	−1300.60	0.076
Cd^{2+}	3.83 (±) 0.05	0.02 (±) 0.04	1.90 (±) 0.08	26.13	−1120.23	0.095	2.12 (±) 0.07	0.01 (±) 0.03	1.17 (±) 0.08	24.68	−1311.98	0.082
Co^{2+}	2.67 (±) 0.01	0.05 (±) 0.01	1.47 (±) 0.07	25.28	DNC	0.087	2.22 (±) 0.10	0.01 (±) 0.04	1.48 (±) 0.02	24.81	DNC	0.090
Cu^{2+}	15.34 (±) 0.02	9.95 (±) 0.06	10.56 (±) 0.03	29.56	−1268.29	0.017	9.27 (±) 0.19	3.04 (±) 0.02	3.63 (±) 0.01	28.34	−1460.04	0.013
Mg^{2+}	1.35 (±) 0.02	1.13 (±) 0.07	0.49 (±) 0.16	23.56	−1073.10	0.084	2.07 (±) 0.09	0.37 (±) 0.11	1.05 (±) 0.06	24.63	−1264.85	0.071
Ni^{2+}	3.01 (±) 0.01	0.13 (±) 0.03	1.41 (±) 0.13	25.51	−1241.44	0.083	4.97 (±) 0.02	0.03 (±) 0.19	0.16 (±) 0.13	21.09	−1433.19	0.092
Zn^{2+}	2.48 (±) 0.01	0.02 (±) 0.24	1.51 (±) 0.09	25.05	−1072.78	0.077	2.18 (±) 0.07	0.01 (±) 0.07	1.07 (±) 0.19	24.75	−1329.53	0.079
Na^{+}	2.05 (±) 0.04	ND	0.95 (±) 0.05	24.60	−1137.78	0.094	4.48 (±) 0.14	0.03 (±) 0.08	1.58 (±) 0.09	26.54	−1433.19	0.064
Li^{+}	2.94 (±) 0.01	0.09 (±) 0.14	1.35 (±) 0.01	25.45	−1080.11	0.082	1.29 (±) 0.12	0.71 (±) 0.02	1.28 (±) 0.07	25.52	−1264.52	0.076

[a] The fluorescence quantum yields (Φ_f) were determined by comparing the integrated fluorescence spectra of the sample with Tryptophan in buffer ($\Phi_f = 0.14$) [53–55]

[b] The Stern–Volmer constant K_{sv} and association constant K_a were determined by linear fitting of fluorescence data using Stern–Volmer equation and its modified version respectively [51, 52]

ND Association constant not determined due to weak interactions

DNC Did not converge

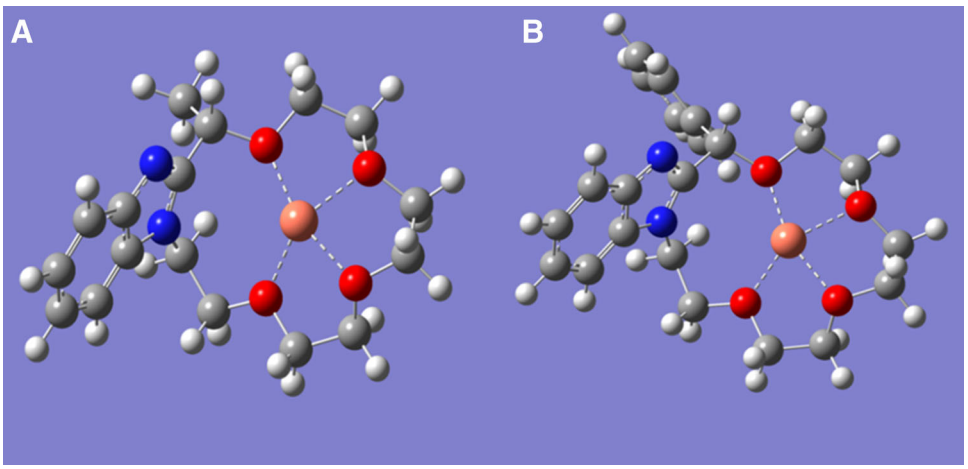

Fig. 7 Copper complexes of azacrown **3** (**a**) and **4** (**b**) respectively

the absorbance intensity gradually increased upon addition of Cu^{2+} ions at their characteristic absorption wavelength of 254 nm, thus eliminating the scope of dynamic quenching. Static quenching process typically yields changes in the absorption profile, [70–73] which is evident in our case. We hypothesize that, probably the groove between benzimidazole and azacrown junction, where we propose our receptor to accommodate the analyte cation, is not easily accessible to facilitate collisional or dynamic quenching, due to steric crowding, thus validating the dominance of static quenching model for receptors **3** & **4** during complexation.

Thus receptors **3** & **4** in the company of Cu^{2+} follow a sphere of action static quenching model, indicating the formation of a dark/non-fluorescent complex. The spectrophotometric titration profile is devoid of any isobestic point, instead only change in absorbance intensity at the intrinsic λ_{max} 254 nm, of the receptor complementing the hypothesis of sphere of action static quenching model operative during the binding events. The dark complex is the consequence of heavy metal effect brought about by Cu^{2+} with unfilled *d*-shell orbitals, coming in the vicinity of benzimidazole fluorophore in the excited state leading to CHEQ effect, via an electron or an energy transfer (ET).

Structural investigation of Cu2+ complexes of azacrowns 3 & 4 (**3**-Cu^{2+} and **4**-Cu^{2+}) by IR spectra

Infrared (IR) spectra were recorded on PerkinElmer Spectrum Version 10.03.07 spectrometer. The samples were prepared in KBr Disks. The bonding of the azacrowns **3** & **4** to the Cu^{2+} ions was studied by IR spectroscopy. FT-IR spectrum of **3** (Fig. SI-1B) showed distinct absorptions of OH, CH and CH_3 at 3,367, 2,923 and 2,853 cm^{-1} respectively. The FT-IR spectrum of **3**-Cu^{2+} showed a considerable shift and broadening of OH absorption band at 3,349 cm^{-1} accompanied by shift of CH absorption band 2,883 cm^{-1}, indicating the involvement of the carbon atom placed at α-position to benzimidazole ring and the substituents attached to it during Cu^{2+} complex formation. Appearance of new bands in the range 1,200–1,011 cm^{-1} for the complexes are due to the presence of perchlorate anion. New bands in the range 470–431 cm^{-1} are obtained for Cu–O. Similarly FT-IR spectrum of **4** (Figure SI-8B) showed distinct absorptions of OH at 3,349 cm^{-1}, aliphatic CH stretching at 2,970 cm^{-1}, bands at 2,931 and 2,881 cm^{-1} due to aromatic CH stretching's were obtained. The FT-IR spectrum of **4**-Cu^{2+} exhibited a broad, shifted absorption bands at 3,406 cm^{-1} attributed to OH and subsided band for CH stretching. The spectrum of **4**-Cu^{2+} complex also showed a shift of absorption bands due to aromatic CH stretching's at 2,922 and 2,876 cm^{-1}, indicating the involvement of the carbon atom placed at α-position to benzimidazole ring and the substituents attached to it during Cu^{2+} complex formation. C=N stretching at 1,647 cm^{-1} observed in the spectrum of uncomplexed **4** was seen to be shifted to lower frequency i.e. 1,615 cm^{-1} in **4**-Cu^{2+} complex spectrum, indicating its involvement during complexation of azacrown 4 with Cu^{2+}. This shifting of the band to lower frequency region is due to decrease in electron density in the C=N region. This confirms the formation of -C=N-Cu bond. Cu–N stretching band in the **4**-Cu^{2+} appears at 487 cm^{-1}. The aromatic C=C stretching's in uncomplexed **4** were shifted form 1,465–1,400 cm^{-1} to higher frequencies i.e. 1,478–1,458 cm^{-1} in **4**-Cu^{2+} confirming the participation of phenyl ring at α-position to benzimidazole in complex formation. Appearance of new bands in the range 1,200–1,011 cm^{-1} for the complexes are due to the presence of perchlorate anion.

DFT based geometry optimization of Metal- azacrown complexes

In order to have a better insight into the mode of interactions of Cu^{2+} with receptors **3** and **4,** DFT calculations were performed using Gaussian 03 W. The metal-azacrown complexes were optimized by the DFT method using the B3LYP density functionals. Numerical integrations were performed using the default grid of Gaussian 03 and the Gaussian 03 default values were chosen for the self-consistent field (SCF) and geometry optimization convergence criteria. For the purpose of optimization of structures, the metal ions Li^{+}, Na^{+}, K^{+}, Ba^{2+}, Cu^{2+}, Ca^{2+}, Mg^{2+}, Cd^{2+}, Zn^{2+}, Co^{2+}, and Ni^{2+} were assigned the basis setsof 'LAN2DZ', which imply the use of Hay and Wadt effective core potentials (ECPs) in combination with their accompanying valence double-ξ basis sets for all elements beyond the first row. Other atoms such as C, H, N were assigned the 6–31 g + (d, p) basis sets. The free energies for the complexes were calculated for the geometry optimized structures (Fig. 7).

The free energies (E_h) for the various optimized metal crown complexes studied are depicted in Table 1. The lowest energy values for Cu^{2+} complexes of both azacrowns **3** and **4** indicate their superior stability in comparison to the other metal ions investigated. From the figures it is evident that copper ion forms coordinate bonds (dotted line) with the crown oxygen atoms having a square planar geometry. The bond lengths between copper ion and oxygen atom range between 2.09 to 2.14 Å.

Conclusion

In conclusion, we have designed a unique class of easily accessible benzimidazole-based azacrown receptors **3** and **4** with selective signaling for detection of Cu^{2+} at biological pH. Both **3** and **4** work as efficient fluorescent probes toward Cu^{2+} in 90 % aqueous medium and validate their utility as a selective Cu^{2+} sensors. Sensor **3** offered a wider and much favorable binding landscape and was found to be a much sensitive probe in comparison to **4**, in which the cation binding site was sterically more crowded. FTIR studies of the azacrowns **3** and **4** in uncomplexed and bound forms ascertain the formation of inclusion complexes with copper. DFT calculations support that Cu^{2+} forms most stable complexes with both the azacrowns **3** and **4**. This study emphasizes the effect of steric environment on receptor sensitivity and its impact on stability of the complex.

Acknowledgments ADP is thankful to UGC-BSR India for financial assistance. Authors are thankful to Dr. Shyamalava Mazumdar and Mrs. Mamata Kombrabail, the Tata Institute of Fundamental Research, for help in fluorescence studies.

References

1. Fabbrizzi, L., Poggi, A.: Sensors and switches from supramolecular chemistry. Chem. Soc. Rev. **24**, 197–202 (1995). doi:10.1039/CS9952400197
2. Robertson, A. Shinkai, S.: Cooperative binding in selective sensors, catalysts and actuators. Coord.Chem. Rev. 205(1), 157–199 (2000). doi:10.1016/S0010-8545(00)00243-5
3. Qi, J., Han, M.S., Ching-Hsuan Tung, C.–H.: A benzothiazole alkyne fluorescent sensor for Cu detection in living cell. Bioorg. Med. Chem. Lett. **22**, 1747–1749 (2012). doi:10.1016/j.bmcl.2011.12.140
4. Brown, E. G. (ed) In: Ring nitrogen and key biomolecules: the biochemistry of N-Heterocycles, The Kluwer Academic Publishers: The Netherlands (1998). doi: 10.1007/978-94-011-4906-8_9
5. Ballesteros, E., Moreno, D., Gómez, T., Rodríguez, T., Rojo, J., Garciá-Valverde, M., Torroba, T.: A new selective chromogenic and turn-on fluorogenic probe for Copper (II) in Water–Acetonitrile 1:1 Solution. Org. Lett. **11**(6), 1269–1272 (2009). doi:10.1021/ol900050z
6. Rurack, K. : Flipping the light switch 'ON'—the design of sensor molecules that show cation-induced fluorescence enhancement with heavy and transition metal ions *Spectrochimi.* Acta Part A **57**(11), 2161–2195 (2001). doi:10.1016/S1386-1425(01)00492-9
7. Czarnik, A.W. (ed). In: *Fluorescent Chemosensors for Ion and Molecule Recognition*, American Chemical Society, Washington (1993)
8. de Silva, A.P., Gunaratne, H.Q.N., Gunnlaugsson, T., Huxley, A.J.M., McCoy, C.P., Rademacher, J.T., Rice, T.E.: Signaling recognition events with fluorescent sensors and switches. Chem. Rev. **97**(5), 1515–1566 (1997). doi:10.1021/cr960386p
9. Valeur, B., Leray, I.: Design principles of fluorescent molecular sensors for cation recognition. Coord. Chem. Rev. 205(1), 3–40 (2000). doi:10.1016/S0010-8545(00)00246-0
10. Prodi, L., Bolletta, F., Montaldi, M., Zaccheroni, N.: Luminescent chemosensors for transition metal ions. Coord. Chem. Rev. 2000, 205, 59–83. doi: 10.1016/S0010-8545(00)00242-3
11. Desvergne, J.P., Czarnik, A.W.: In: Chemosensors of Ion and Molecule Recognition. Kluwer, Dordrecht (1997). doi:10.1007/978-94-011-3973-1_6
12. Hartter, D.E., Barnea, A.: Evidence for release of copper in the brain: depolarization-induced release of newly taken-up 67 copper. Synapse **2**, 412–415 (1988). doi:10.1002/syn.890020408
13. Kardos, J., Kovacs, I., Hajos, F., Kalman M., Simonyi, M.: Nerve endings from rat brain tissue release copper upon depolarization. A possible role in regulating neuronal excitability. Neurosci. Lett. **103**, 139–144 (1989). doi: 10.1016/0304-3940(89)90565-X
14. Que, E.L., Domaille, D.W., Chang, C.J.: Metals in neurobiology: probing their chemistry and biology with molecular imaging. Chem. Rev. **108**(5), 1517–1549 (2008). doi:10.1021/cr078203u
15. McRae, R., Bagchi, P., Sumalekshmy, S., Fahrni, J.C.: In situ imaging of metals in cells and tissues. Chem. Rev. **109**(6), 4780–4827 (2009). doi:10.1021/cr900223a
16. Mathie, A., Sutton, G.L., Clarke, C.E., Veale, E.L.: Zinc and copper: pharmacological probes and endogenous modulators of neuronal excitability. Pharm. Ther. **111**(3), 567–583 (2006). doi:10.1016/j.pharmthera.2005.11.004
17. Haliwell, B., Gutteridge, J.M.C.: Oxygen toxicity, oxygen radicals, transition metals and disease. Biochem. J. **219**, 1 (1984).

18. Muthaup, G., Schlicksupp, A., Hess, L., Beher, D., Ruppert, T., Masters, C.L., Beyreuther, K.: The amyloid precursor protein of alzheimer's disease in the reduction of Copper(II) to Copper(I). Science **271**, 1406 (1996). doi:10.1126/science.271.5254.1406
19. Løvstad, R.A.: A kinetic study on the distribution of Cu(II)-ions between albumin and transferrin. Biometals **17**(2), 111–113 (2004). doi:10.1023/b:biom.0000018362.37471.0b
20. Singh, N., Kaur, N., McCaughan, B., Callan, J. F.: Ratiometric fluorescent detection of Cu(II) in semi-aqueous solution using a two-fluorophore approach. Tet. Lett. **51**(26), 3385–3387 (2010). doi:10.1016/j.tetlet.2010.04.099
21. E. L. Que, D. W. Domaille and Chang, C. J. Metals in neurobiology: probing their chemistry and biology with molecular imaging. Chem. Rev. **108**(5), 1517–1549 (2008). doi:10.1021/cr078203u
22. Miller, E.W., Zeng, L., Domaille, D.W., Chang, C.J.: Preparation and use of Coppersensor-1, a synthetic fluorophore for live-cell copper imaging. Nat. Protoc. **1**, 824–827 (2006). doi:10.1038/nprot.2006.140
23. Kaur N., Kumar, S.: Colorimetric recognition of Cu(II) by (2-dimethylaminoethyl)amino appended anthracene-9,10-diones in aqueous solutions: deprotonation of aryl amine NH responsible for colour changes. Dalton Trans. 3766–3771 (2006)
24. Khatua, S., Choi, S.H., Lee, J., Huh, J.O., Do, Y., Churchill, D.G.: Highly selective fluorescence detection of Cu^{2+} in water by chiral dimeric Zn^{2+} Complexes through direct displacement. Inorg. Chem. **48**, 1799–1801 (2009). doi:10.1021/ic802314u
25. Kramer, R.: Fluorescent chemosensors for Cu^{2+} Ions: fast, selective, and highly sensitive. Angew. Chem. Int. Ed. **37**, 772–773 (1998). doi:10.1002/(SICI)1521-3773(19980403
26. Gunnlaugsson, T., Leonard J. P., Murray, N. S.: Highly selective colorimetric naked-eye Cu(II) detection using an azobenzene chemosensor. Org. Lett. **6**(10), 1557–1560 (2004). doi:10.1021/ol0498951]
27. Lin, W., Long, L., Chen, B., Tan, W., Gao, W.: Fluorescence turn-on detection of Cu^{2+} in water samples and living cells based on the unprecedented copper-mediated dihydrorosamine oxidation reaction. Chem. Commun. **46**, 1311–1313 (2010). doi:10.1039/B919531A
28. Xu, Z., Han, S.J., Lee, C., Yoon, J., Spring, D.R.: Development of off–on fluorescent probes for heavy and transition metal ions. Chem. Commun. **46**, 1679–1681 (2010). doi:10.1039/B924503K
29. Konishi, K., Hiratani, T.: Turn-on and selective luminescence sensing of copper ions by a water-soluble $Cd_{10}S_{16}$ molecular cluster. Angew. Chem. Int. Ed. **45**, 5191–5194 (2006). doi:10.1002/anie.200601491
30. Li, G. -K., Xu, Z. -X., Chen, C. -F., Huang, Z. -T.: A highly efficient and selective turn-on fluorescent sensor for Cu^{2+} ion based on calix[4]arene bearing four aminoquinoline subunits on the upper rim. Chem. Commun. 1774–1776 (2008). doi: 10.1039/B800258D
31. Khatua, S., Kang, J., Churchill, D.G.: Direct dizinc displacement approach for efficient detection of Cu^{2+} in aqueous media: acetate *versus* phenolate bridging platforms. New J. Chem. **34**, 1163–1169 (2010). doi:10.1039/B9NJ00770A
32. Xu, Z., Qian, X., Cui, J.: J.: colorimetric and ratiometric fluorescent chemosensor with a large red-shift in emission: Cu(II)-only sensing by deprotonation of secondary amines as receptor conjugated to naphthalimide fluorophore. Org. Lett. **7**(14), 3029–3032 (2005). doi:10.1021/ol051131d
33. Karnik, A.V., Mirgane, N.A.: Asymmetric Diels-Alder reaction involving chiral benzimidazoles as organocatalysts. Chirality **23**(5), 404–407 (2011). doi:10.1002/chir.20942
34. Karnik, A.V., Mirgane, N.A.: Aqueous ethanol: a suitable medium for the diastereoselective Diels-Alder reaction mediated by chiral bases. Green Chem. Lett. Rev. **4**(3), 269–272 (2011). doi:10.1080/17518253.2011.571715
35. Mirgane, N.A., Karnik, A.V., Akhtar, M.H.: Chiral ionic liquid mediated diels—alder reaction between anthrone enolate and maleimides. Lett. Org. Chem. **7**(4), 343 (2010)
36. Pandey, A. D., Mohammed H., Karnik, A. V.: Chiral benzimidazole-derived mono azacrowns: synthesis and enantiomer recognition studies with chiral amines and their ammonium salts. Tet: Asym. **24**, 706–712 (2013). doi:10.1016/j.tetasy.2013.04.021
37. Karnik, A.V., Kamath, S.S.: Enantioselective benzoylation of a-amino esters using (S)-1-Benzoyl-2- (α-acetoxyethyl)benzimidazole, a chiral benzimidazolide. J. Org. Chem. **72**, 7435 (2007). doi:10.1021/jo070962p
38. Karnik, A.V., Kamath, S.S.: Enantioselective benzoylation of racemic amines using chiral benzimidazolide as a benzoylating agent. Tetrahedron: Asym. **19**, 45 (2008). doi:10.1016/j.tetasy.2007.12.006
39. Katritzky, A. R., Fedoseyenko, D., Kim, M. S., Steel, P. J.: Chiral 1,2,4-triazoles: stereoselective acylation and chlorination Tetrahedron: Asym. **21**(1), 51–57 (2010). doi:10.1016/j.tetasy.2009.12.007
40. Phillips, M. A.: The formation of 2-substituted benziminazoles. J. Chem. Soc. 2393-2399 (1928). doi: 10.1039/JR9280002393
41. Katrizky, A. R., Aslan, D. C., Leeming, P., Steel, P. J.: Stereoselective synthesis of 2-(α-hydroxyalkyl)benzimidazoles. Tetrahedron: Asym. **9**(13), 2245-2251 (1998). doi:10.1016/S0957-4166(98)00202-X
42. Gokel, G. W., Leevy, W. M., Weber, M. E.: Crown ethers: sensors for ions and molecular scaffolds for materials and biological models. Chem. Rev. **104**(5), 2723–2750 (2004). doi: 10.1021/cr020080k
43. Bünzli, J.-C.G., Piguet, C.: Taking advantage of luminescent lanthanide ions. Chem. Soc. Rev. **34**, 1048 (2005). doi:10.1039/B406082M
44. Bakó, T.; Bakó, P.; Keglevich, G.; Makó B. A.; Tóke, L.: The enantiomeric recognition of chiral organic ammonium salts by chiral monoaza-15-crown-5 ether derivatives. Tetrahedron: Asym. **15**(10), 1589–1595 (2004). doi:10.1016/j.tetasy.2004.03.035
45. Huszthy, P., Oue, M., Bradshaw, J.S., Zhu, C.Y., Wang, T., Curtis, J.C., Izatt, R.M.: New symmetrical chiral dibenzyl- and diphenyl-substituted diamido-, dithionoamido-, diaza-, and azapyridino-18-crown-6 ligands. J. Org. Chem. **57**(20), 5383–5394 (1992). doi:10.1021/j000046a020
46. Ménand, M., Blais, J.C., Xie, J.: De novo synthesis of sugar-aza-crown ethers via a domino Staudinger aza-Wittig reaction. J. Org. Chem. **71**(8), 3295–3298 (2006). doi:10.1021/jo052489q
47. Zhang, G.M., Brown, H.C., Ramachandran, P.V.: Chiral synthesis via organoboranes. 46. An efficient preparation of Chiral Pyridino- and Thiopheno-18-crown-6 ligands from enantiomerically Pure C_2-Symmetric Pyridine- and Thiophenediols. J. Org. Chem. **64**, 721–725 (1999). doi:10.1021/jo980899r
48. Nazhaoui, M., Joly, J. P., Kitane, S., Berrada, M.: 1,6-Dideoxy-D-mannitol-based 20-crown-6 ethers: synthesis and influence of the substituents upon complexing properties toward phenylglycinium methyl esters. J. Chem. Soc., Perkin Trans. 1 **22**(1), 3845–3850 (1998)**.** doi: 10.1039/A804873H
49. Huszthy, P., Bradshaw, J.S., Zhu, C.Y., Izatt, R.M.: Recognition by new symmetrically substituted chiral diphenyl- and di-tert-butylpyridino-18-crown-6 and asymmetrically substituted chiral dimethylpyridino-18-crown-6 ligands of the enantiomers of various organic ammonium perchlorates. J. Org. Chem. **56**(10), 3330–3336 (1991). doi:10.1021/jo00010a028
50. Lakowicz, J. R.: Principles of Fluorescence Spectroscopy, 3rd edn., Plenum: New York, USA, 54–57 (2006)

51. Lakowicz, J. R.: Principles of Fluorescence Spectroscopy, 2nd edn., Plenum: New York, USA, 1999; pp 277–283
52. Eftink, M. R.: Fluorescence methods for studying equilibrium macromolecule-ligand interactions. Methods Enzym., **278**, 221–257 (1997). doi:10.1016/S0076-6879(97)78013-3
53. Kirby, E.P., Steiner, R.F.: Influence of solvent and temperature upon the fluorescence of indole derivatives. J. Phys. Chem. **74**, 4480 (1970). doi:10.1021/j100720a004
54. Chen, R.F.: fluorescence quantum yields of tryptophan and tyrosine. Anal. Lett. **1**(1), 35–42 (1967). doi:10.1080/00032716708051097
55. Creed, D.: The photophysics and photochemistry of the near-uv absorbing amino acids–i. Tryptophan and its simple derivatives. Photochem. Photobiol. **39**(4), 537–562 (1984). doi:10.1111/j.1751-1097.1984.tb03890.x
56. Liu, J., Lu, Y.: A DNAzyme catalytic beacon sensor for paramagnetic Cu^{2+} ions in aqueous solution with high sensitivity and selectivity. J. Am. Chem. Soc. **129**(32), 9838–9839 (2007). doi:10.1021/ja0717358
57. Qi, X., Jun, E.J., Xu, L., Kim, S.-J., Hong, J.S.J., Yoon, Y.J., Yoon, J.: New BODIPY derivatives as OFF–ON fluorescent chemosensor and fluorescent chemodosimeter for Cu2 + : cooperative selectivity enhancement toward Cu2+. J. Org. Chem. **71**(7), 2881–2884 (2006). doi:10.1021/jo052542a
58. Rurack, K., Kollmannsberger, M., Resch-Genger, U., Daub, J.: A selective and sensitive fluoroionophore for Hg^{II}, Ag^{I}, and Cu^{II} with virtually decoupled fluorophore and receptor units. J. Am. Chem. Soc. **122**(5), 968–969 (2000). doi:10.1021/ja992630a
59. Kim, S.H., Kim, J.S., Park, S.M., Chang, S.-K.: Hg^{2+}-selective OFF–ON and Cu^{2+}-Selective ON–OFF type fluoroionophore based upon cyclam. Org. Lett. **8**(3), 371–374 (2006). doi:10.1021/ol052282j
60. Kim, H. J., Park, S. Y.; Yoon S., Kim, J. S.: FRET-derived ratiometric fluorescence sensor for Cu^{2+}. Tetrahedron **64**(7), 1294–1300 (2008). doi:10.1016/j.tet.2007.11.063
61. Z.-Q., Guo, Chen W.-Q., Duan, X.-M.: Highly selective visual detection of Cu(II) utilizing intramolecular hydrogen bond-stabilized merocyanine in aqueous buffer solution. Org. Lett. **12**(10), 2202–2205 (2010). doi: 10.1021/ol100381g
62. Huang, J., Xu, Y., Qian, X.: A red-shift colorimetric and fluorescent sensor for Cu^{2+} in aqueous solution: unsymmetrical 4,5-diaminonaphthalimide with N-H deprotonation induced by metal ions. Org. Biomol. Chem. **7**, 1299–1303 (2009). doi:10.1039/B818611A
63. Xu, Z., Pan, J., Spring, D. R., Cui J., Yoon, J.: Ratiometric fluorescent and colorimetric sensors for Cu^{2+} based on 4,5-disubstituted-1,8-naphthalimide and sensing cyanide via Cu^{2+} displacement approach. Tetrahedron **66**(9), 1678–1683 (2010). doi:10.1016/j.tet.2010.01.008
64. Durgadas, C.V., Sharma, C.P., Sreenivasan, K.: Fluorescent gold clusters as nanosensors for copper ions in live cells. Analyst **136**, 933–940 (2011). doi:10.1039/C0AN00424C
65. Jung, H.S., Park, M., Han, D.Y., Kim, E., Lee, C., Ham, S., Kim, J.S.: Cu^{2+} ion-induced self-assembly of pyrenylquinoline with a pyrenyl excimer formation. Org. Lett. **11**(15), 3378–3381 (2009). doi:10.1021/ol901221q
66. Jun Feng Zhang: Ying Zhou, Juyoung Yoon, Youngmee Kim, Sung Jin Kim and Jong Seung Kim: Naphthalimide modified rhodamine derivative: ratiometric and selective fluorescent sensor for Cu2+ based on two different approaches. Org. Lett. **12**(17), 3852–3855 (2010). doi:10.1021/ol101535s
67. Jung, H.S., Han, J.H., Kim, Z.H., Kang, C., Kim, J.S.: Coumarin-Cu(II) ensemble-based cyanide sensing chemodosimeter. Org. Lett. **13**(19), 5056–5059 (2011). doi:10.1021/ol2018856
68. Jung, H.S., Park, M., Han, J.H., Lee, J.H., Kang, C., Jung, J.H., Kim, J.S.: Selective removal and quantification of Cu(II) using fluorescent iminocoumarin-functionalized magnetic nanosilica. Chem. Commun. **48**, 5082–5084 (2012). doi:10.1039/C2CC18113D
69. Lee, Y.H., Park, N., Park, Y.B., Hwang, Y.J., Kang, C., Kim, J.S.: Organelle-selective fluorescent Cu^{2+} ion probes: revealing the endoplasmic reticulum as a reservoir for Cu-overloading. Chem. Commun. **50**, 3197–3200 (2014). doi:10.1039/C4CC00091A
70. Lakowicz, J. R.: Principles of fluorescence spectroscopy. 3. Springer; New York: 2006
71. Jiang, C. Q., Wang T.: Study of the interactions between tetracycline analogues and lysozyme Bioorg. & Med. Chem. 12, 2043–2047, 2004. doi: 10.1016/j.bmc.2004.02.035
72. Lee, D.Y., Singh, N., Kim, M.J., Jang, D.O.: Chromogenic and fluorescent recognition of iodide with a benzimidazole-based tripodal receptor. Org. Lett. **13**(12), 3024–3027 (2011). doi:10.1021/ol2008846
73. Vetrichelvan, M., Nagarajan, R., Valiyaveettil, S.: Carbazole-containing conjugated copolymers as colorimetric/fluorimetric sensor for iodide anion. Macromolecules **39**(24), 8303–8310 (2006). doi:10.1021/ol2008846